Sensors and Materials, Vol. 29, No. 8 (2017) 1213–1222
MYU Tokyo

S & M 1413

Space Charge Distribution in Polymethyl Methacrylate and Quartz Glass Irradiated by Protons

Hiroaki Miyake* and Yasuhiro Tanaka

Tokyo City University, 1-28-1 Tamazutsumi, Setagaya-ku, Tokyo 158-8557, Japan

(Received January 13, 2017; accepted May 2, 2017)

Keywords: spacecraft, space environment, proton, space charge, PEA

Many satellites are used in several kinds of orbits for telecommunications, environmental observation, resource exploration, the global positioning system, and social security. These satellites are always exposed to radiations, such as electrons and protons. Charged particles accumulate in the bulk of the surface materials of spacecraft and lead to electrostatic discharge (ESD) phenomena. ESD is the origin of satellite anomalies; hence, we should investigate charge accumulation phenomena in the bulk of satellites surface materials. In this study, we focused on the charge accumulation phenomena in polymethyl methacrylate (PMMA) and highly purified quartz glass using the pulsed electroacoustic (PEA) method. From our study, we could confirm the positive charge accumulation in the materials irradiated by protons except for the case of a quartz glass with an Al evaporated layer on the irradiated side. From the results, we considered the reasons that the positive charge accumulated in PMMA and quartz glass while no charge accumulated in the quartz glass with the Al evaporated layer.

1. Introduction

Currently, the demand for the use of satellites is continually increasing for telecommunications, environmental observation, resource exploration, the global positioning system, and social security. Satellites are operated during orbit, where many radiations exist, for example, electrons, protons, and γ-rays.[1] Such high-energy charged particles are irradiated and accumulate in satellites' surface materials. Because of this, many polymeric materials and glasses are used as surface materials for satellites. For example, polyimide films are used for multilayer insulators (MLIs), and glasses are used as coverings for photovoltaic (PV) cells. Consequently, voltage potential differences were produced by these charged particles between surface materials and the base structure of satellites or other surface materials.

This accumulation is the origin of discharge phenomena. Those discharge phenomena may be the possible origin of satellite operational anomalies. Figure 1 shows the origin of satellite anomalies on commercial satellites defined by Koons *et al.*[2] From the figure, we see that electrostatic discharge (ESD) is the origin of more than 50% of satellite anomalies. Furthermore, as an example of an accident involving a Japanese satellite, a power outage occurred in the Advanced Earth-Observing Satellite-II (ADEOS-II, also called Midori-2) due to ESD.[3] To prevent such accidents and ensure the high reliability of satellite operations, we need to investigate

*Corresponding author: e-mail: hmiyake@tcu.ac.jp
http://dx.doi.org/10.18494/SAM.2017.1574

ISSN 0914-4935

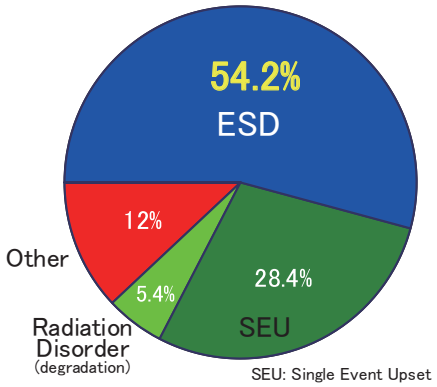

Fig. 1. (Color online) Origin of satellite anomalies.

the charging and discharging characteristics of surface materials of satellites exposed to radiations.

To date, many researchers have studied the characteristics of charge accumulation in a few dielectrics exposed to electron beam irradiation.[4–7] However, no one has studied the characteristics of charge accumulation in proton-irradiated materials. We are studying the characteristics of charge accumulation in dielectrics in satellites irradiated by protons. In this paper, we focus on the charge accumulation phenomena in polymethyl methacrylate (PMMA) and highly purified quartz glass using the pulsed electroacoustic (PEA) method. PMMA is a reference material for space charge measurements using the PEA method, and quartz glass is the base material in cover glasses for PV cells. We and other researchers have considerable experience in measuring the space charge distribution in materials irradiated by electrons as reference materials in the PEA method.[6–8] Furthermore, no one has reported charge accumulation phenomena in dielectrics irradiated by protons. We have initiated studies of charge accumulation phenomena in PMMA and quartz glass dielectrics irradiated by protons.

From the results, we confirmed positive charge accumulation within those materials. However, we could not confirm the presence of any charges in quartz glass with an Al evaporated layer on the irradiation surface. In this paper, we introduce and discuss the results of space charge distribution in the bulk of those materials.

2. Experimental Procedures

2.1 Sample

PMMA and highly purified quartz glass are used as samples. The size of the samples is 30×30 mm^2 and their thickness is about 1.0 mm. We prepared those samples with and without an Al evaporated layer on the irradiation surface. During proton beam irradiation, the Al evaporated layer was connected to ground. Furthermore, for the space charge measurement during irradiation, PMMA with a thickness of 125 μm was used. This sample also has an Al evaporated layer on the irradiation surface. The thickness of the eveporated layer is approximately 300 Å.

2.2 Conditions for preparation of irradiated samples and space charge measurement procedures

Proton beam irradiation was carried out under a vacuum of approximately 1×10^{-5} Pa. The acceleration energy of the irradiated proton was 1.0, 3.0, or 6.0 MeV. The current density is shown in Table 1.

The current density is different between quartz glass and PMMA samples because the glass transition temperature of PMMA is lower than that of the glass. Because PMMA may melt due to heat from irradiation, we chose a lower current density compared with that applied to the quartz glass. However, we adjust the current density and irradiation time to ensure the same fluence for each irradiation.

Different current densities for each sample of PMMA and glass enable us to suppress thermal damage to PMMA due to proton beam irradiation current. Consequently, we control the total amount of proton fluence on each sample.

After irradiation, we measured the space charge distribution using the PEA method under short circuit conditions. Measurements on PMMA samples were performed 1 d after irradiation; for quartz glass samples, measurements were performed 5 d after irradiation to protect the person inspecting the sample from radiation exposure. Our irradiated samples were normally activated due to the proton irradiation. Those samples were held in a chamber until the dose from radioactive samples returned to the background level. Therefore, we allowed 5 d to elapse before the quartz glass samples were taken out of the radiation-controlled area.

2.3 Conditions for in-site space charge measurements under irradiation

With respect to space charge measurements during irradiation, we carried out irradiation using protons with an energy of 1.5 MeV and a current of either 3 or 30 nA/cm^2. The irradiation time was 60 min. PMMA samples with a thickness of 125 mm and evaporated Al on their surfaces were used. Those samples were set to the PEA apparatus for irradiation with the Al surface set as the irradiation side.

2.4 Irradiation facilities

The irradiation was carried out using the 3 MeV Tandem Accelerator facility of Takasaki Advanced Radiation Research Institute of the National Institutes for Quantum and Radiological Science and Technology, Japan (its former name was the Japan Atomic Energy Agency) and the 3.75 MV Van de Graff of High Fluence Irradiation Facility at the University of Tokyo. We measured the charge distribution in the samples after irradiation in air atmosphere. All measurements were carried out at room temperature (approximately 293 K).

Table 1
Irradiation conditions for each sample.

Sample	Current density (nA/cm^2)	Irradiation time (min)	Fluence (cm^{-2})
PMMA	3	30	5.63 E+11
Quartz glass	30	3	5.63 E+11

2.5 System and procedures for space charge measurement

The space charge measurement was carried out during 60 min of irradiation followed by 10 min of relaxation at 30 s intervals under a vacuum of 10^{-5} Pa. The proton accelerator was the same as described previously. The PEA system used in this research was designed and developed specially for the proton irradiation facility.[4,9] Figure 2 shows the photo and schematic diagram of the detecor used in the PEA method. The ring electrode is used as the electrode on the irradiation side, and the irradiated particles reach the sample directly. The ring electrode is connected to the Al layer. We apply a pulsed voltage to the sample to obtain the charge profile. The size of the unit is 68 × 48 × 24 mm^3; this setup was developed based on the assumption that it will be mounted on satellites.[9]

3. Results

Figure 3 shows the space charge distribution in proton-irradiated PMMA and quartz glass with and without an Al evaporated layer. These measurements were carried out with a short circuit between both electrodes. Concerning those figures, a proton irradiation surface is placed on the right side. Figures 3(A) and 3(B) show the results of space charge distribution in PMMA and quartz glass irradiated under the conditions described in Sect. 2.2, respectively. Columns (a)–(c) show the proton irradiation energy. The arrows in the figure are measurements and the calculated proton penetration depth below the irradiated surface.

3.1 Positive charge accumulation in PMMA

From the results for PMMA in Fig. 3(A), a signal due to positive charge accumulation was observed in the sample. The positions of the positive peaks are 432, 94, and 22 μm from the irradiated surface in PMMA without an Al evaporated layer. In the case of PMMA with an Al evaporated layer, the positive peak signals are observed at 452, 121, and 22 μm from the irradiated surface. As both results show no significant change, the positive peak position is not related to the electrical conductive condition of the sample surface.

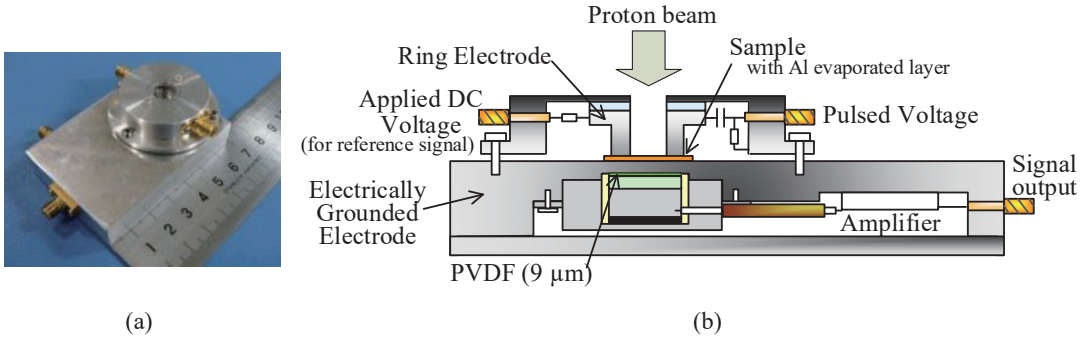

Fig. 2. (Color online) Photo and schematic diagram of PEA measurement apparatus. (a) Photo of sensor unit and (b) schematic diagram of sensor unit used in the PEA method.

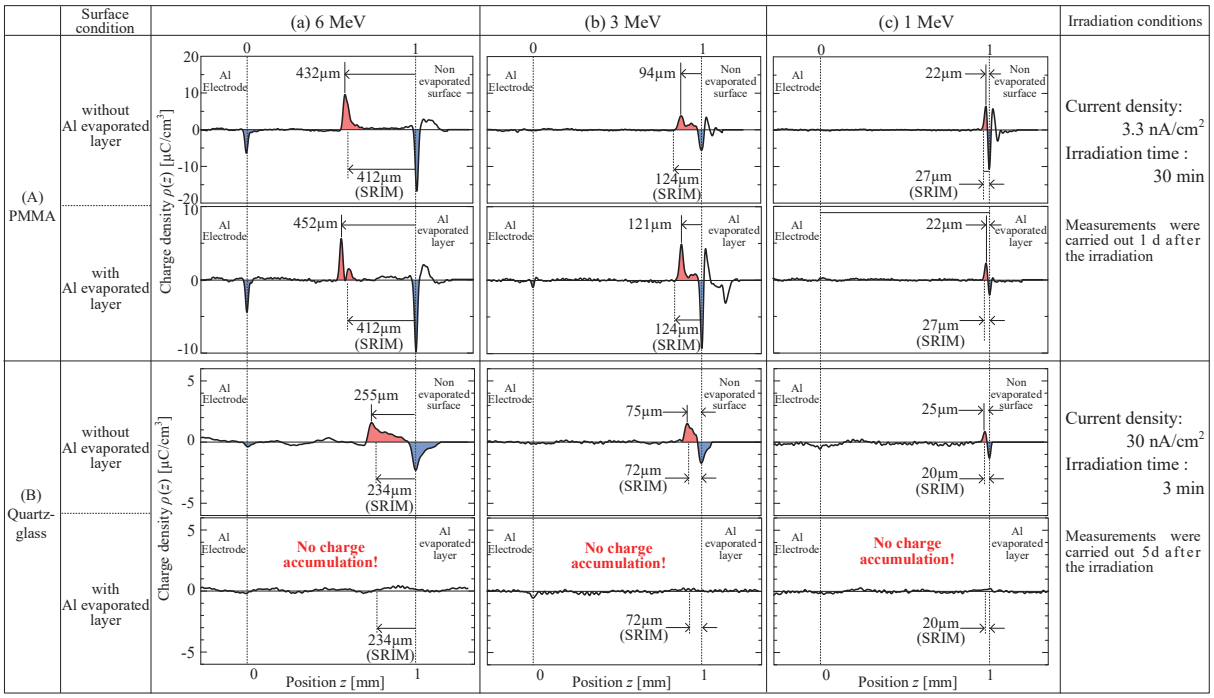

Fig. 3. (Color online) Space charge distribution in PMMA and quartz glass irradiated by protons with monoenergy.

3.2 Positive charge and no charge accumulation in highly purified quartz glass

Space charge distributions in quartz glass irradiated by protons are shown in Fig. 3(B). From the figure, we can see positive charge accumulation in the material without an Al evaporated layer under all irradiation conditions. The positions of the positive peaks at 6, 3, and 1 MeV are 255, 75, and 25 μm, respectively. Furthermore, concerning the differences from the PMMA results, we can also confirm that the positive charges are distributed between the penetration depth and irradiated surface in the quartz glass. However, in quartz glass with an Al evaporated layer, no charge accumulations were observed under all irradiation conditions.

4. Discussion

4.1 Relationship between positive charge accumulation and proton penetration depth

We now discuss the relationship between the position of the positive charge accumulation peak and the proton penetration depth. The proton penetration depth in PMMA and quartz glass can be calculate using the code of the Stopping and Rage of Ions in Matter (SRIM).[10] The calculated penetration depths of PMMA and quartz glass are shown in Table 2. These calculated results are also shown in Fig. 3. Based on the comparison between the calculated penetration depth and position of positive charge accumulated from Fig. 3, proton penetration depth correlates well with the peak for positive charge accumulation. We compared the calculated depth and the charge accumulation position at each energy. The results are shown in Fig. 4. In the figure, the proton irradiation energy and the calculated depth/position of positive charge accumulation are shown in the horizontal and perpendicular axes, respectively. Circles and squares show the position of

Table 2
Calculated penetration depth using SRIM.

Sample	Calculated penetration depth (μm)		
	6 MeV	3 MeV	1 MeV
PMMA	412	124	27
Quartz glass	234	72	20

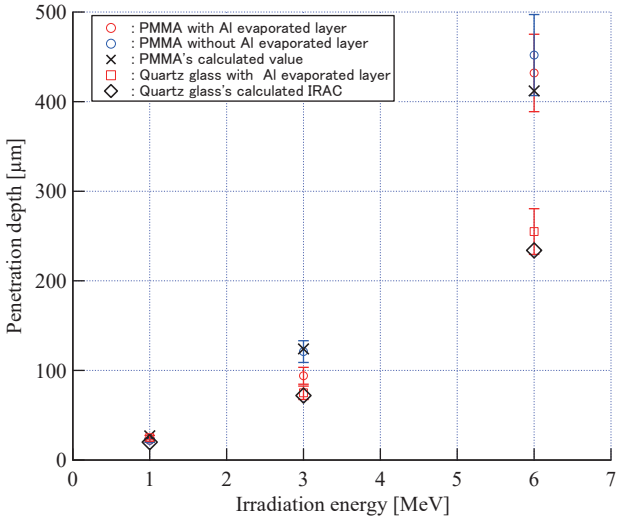

Fig. 4. (Color online) Relationship between position of positive charge accumulation and calculated penetration depth.

charge accumulation from Fig. 3 for PMMA and quartz glass; crosses and diamonds show the calculated proton penetration depths in PMMA and quartz glass, respectively. Red and blue colors correspond to the presence and absence of the Al evaporated layer on the irradiated surface.

Makers for the position of charge accumulation are also shown with error bars based on the 10% spatial resolution of our measurement system.[5,6] From the figure, the calculated penetration depths are within the error bar for all charge accumulation positions except for those of PMMA with an Al evaporated layer at 3 MeV irradiation. Therefore, it is assumed that those positive charge accumulation peaks were produced due to irradiated proton particles.

4.2 No charge accumulation in quartz glass with an Al evaporated layer

Concerning the charge accumulation in quartz glass with an Al evaporated layer on the irradiation surface, in Fig. 3(B), we did not observe any charges in the quartz glass with an Al evaporated layer. We considered two possibilities to explain these results.

To understand the phenomena, it is helpful to consider the results of charge accumulation in quartz glass with an Al evaporated layer when irradiated by electrons, namely, that no charge accumulation was observed in quartz glass.[4] Figure 5 shows a model of energy bands for highly purified quartz glass with an Al evaporated layer on the irradiation surface when it is sandwiched by electrodes. In this figure, E_v represents the energy level of the valence band. E_c, the energy level of the conduction band, and E_f, the Fermi level. From Fig. 5(a), because the injected electrons have high energy and are always in a conduction band, they move freely. Because we used the

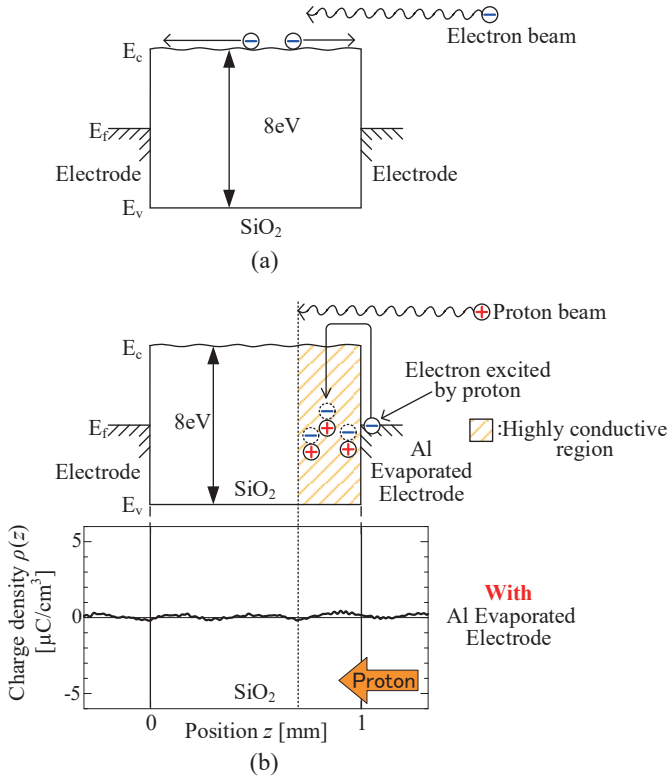

Fig. 5. (Color online) Model of energy bands in quartz glass with an Al evaporated layer. (a) No charge accumulation in quartz glass irradiated by electrons and (b) no charge accumulation in quartz glass irradiated by protons.

same grade of quartz glass for this research, the considerations from our previous work may be adapted to the observation herein of no charge accumulation in quartz glass irradiated by protons. The energy band model for proton-irradiated quartz glass is shown in Fig. 5(b), which includes the space charge result in the quartz glass with an Al evaporated layer irradiated by 6 MeV protons. When high-energy protons were irradiated, the injected protons were trapped in the glass. At that time, because high-energy protons passed through the evaporated layer, some high-energy secondary electrons were also produced in the cross-sectional area of the Al evaporated layer. Such secondary electrons were also injected and drifted toward the accumulated protons in the material. The drift current was driven by the electric field produced by the accumulated protons. Thus, since the drifted electrons were compensated for by the accumulated protons, no charge accumulation was observed.

With respect to the other possibility, the radiation-induced conductivity (RIC) produced by the irradiated high-energy protons produced a highly conductive region in the area passed through by the protons. The RIC area is shown in Fig. 5(b) using orange hatching. RIC areas produced by irradiated protons on other materials have already been reported.[11–14] The RIC produced quite a highly conductive region, as some excited secondary electrons might be injected to the material and might drift toward the position of proton accumulation. The accumulated protons were compensated for by the injected and drifting electrons.

For these reasons, no charges could be observed in the quartz glass with an Al evaporated layer. In either case, as the above possibilities are our suggestions, we need further study to understand the phenomena clearly.

5. In-site space charge measurement under proton irradiation

We carried out space charge measurements under proton irradiation. This time, we focused on PMMA for this in-site measurement in the irradiation chamber. The details of measurement conditions were already described in Sects. 2.3–2.5.

The results for 1.5 MeV with 3 nA/cm^2 irradiation are shown in Fig. 6. From Fig. 6(a), we can see positive charge accumulation as in Fig. 3. From Fig. 6(c), we can see positive charges saturated at a value of about 0.3 mC/m^2 within 10 min after starting the irradiation. Those accumulated charges decreased to about 0.28 mC/m^2 15 min after the irradiation began and maintained the same accumulation value up to the end of the irradiation. After the irradiation, the positive accumulated charges decreased to half initial value. From Fig. 6(d), we can clearly observe the phenomena of charge accumulation during and after irradiation. From the figure, we see the charge accumulation positions shift toward the right side during irradiation. It should be noted that the sample was heated due to proton irradiation. We have already attempted to measure sample surface temperature during irradiation using an IR camera at a preliminary examination in other research. The sample surface reached more than 100 °C for irradiation conditions of 1 MeV and 30 nA/cm^2.

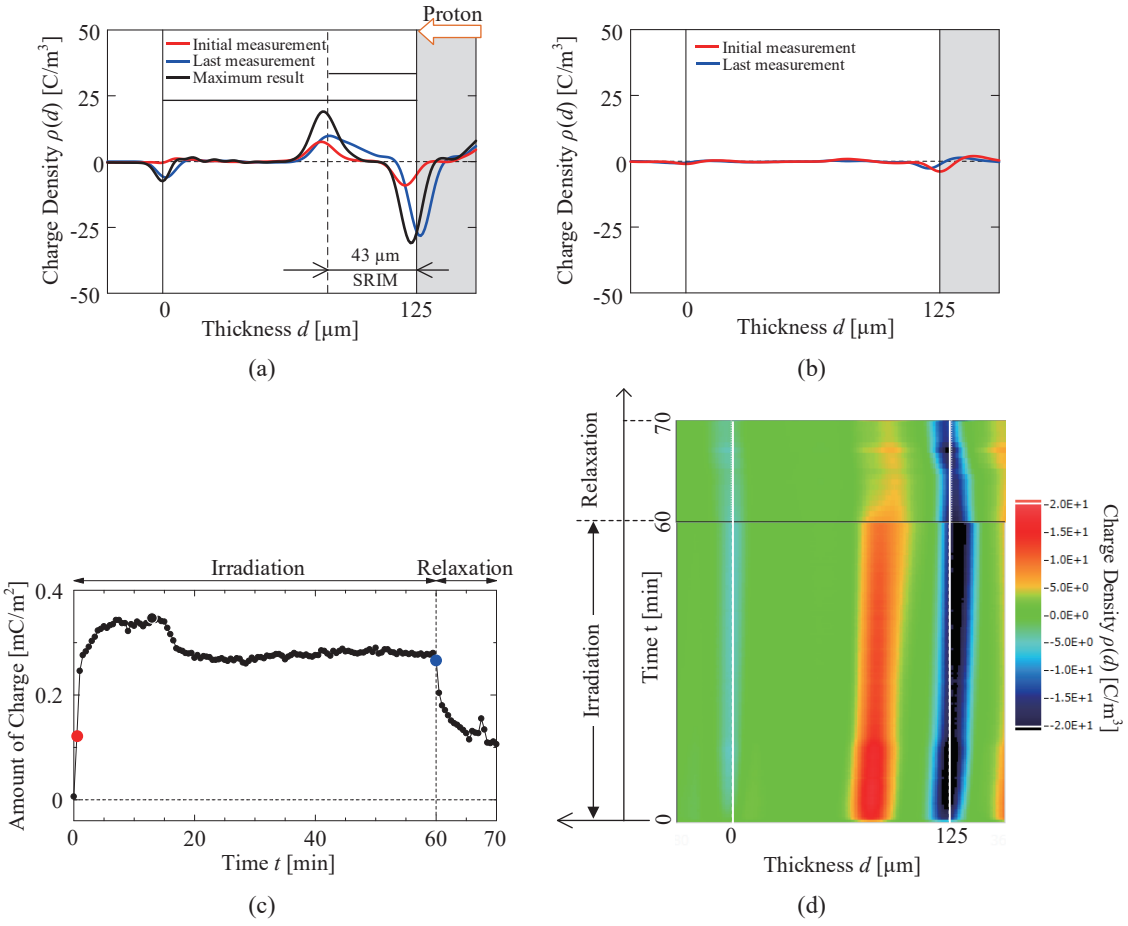

Fig. 6. (Color online) Results of space charge measurement on PMMA during and after proton beam irradiation at 1.5 MeV and 3 nA/cm^2. (a) Space chrnge distribution during irradiation, (b) space charge distribution after irradiation, (c) integrated accumulated positive charges in the material with time, and (d) space charge distribution with time on color chart.

Since the irradiation energy used in this research is higher than those in other studies, the temperature of the irradiated surfaces in this experiment was also higher than 100 °C.

With respect to other studies, we initially used the Tandetron that was installed at the High Fluence Irradiation Facility at the University of Tokyo. The use of the facility was suspended due to the Great East Japan Earthquake. We could obtain the surface temperature quite easily at this facility because we could access the irradiation chamber during irradiation because of the low maximum irradiation energy. To confirm the temperature increase phenomenon on the sample surface during irradiation, we must seek other opportunities to use the irradiation facility.

The results from the 30 nA/cm^2 irradiation are shown in Fig. 7. From the figure, we can see that the accumulated charges saturated until 240 s after initiating irradiation. After 390 s from the start of irradiation, those accumulated charges suddenly decreased. After 30 min, as the positive charges did not increase, the proton irradiation was stopped. After the irradiation, we confirmed erosion at the sample surface. A photo of the sample is shown in Fig. 8. The red broken line shows the irradiated area. We suggest that the reason why charges disappeared during irradiation is that the material melted due to the irradiated protons.

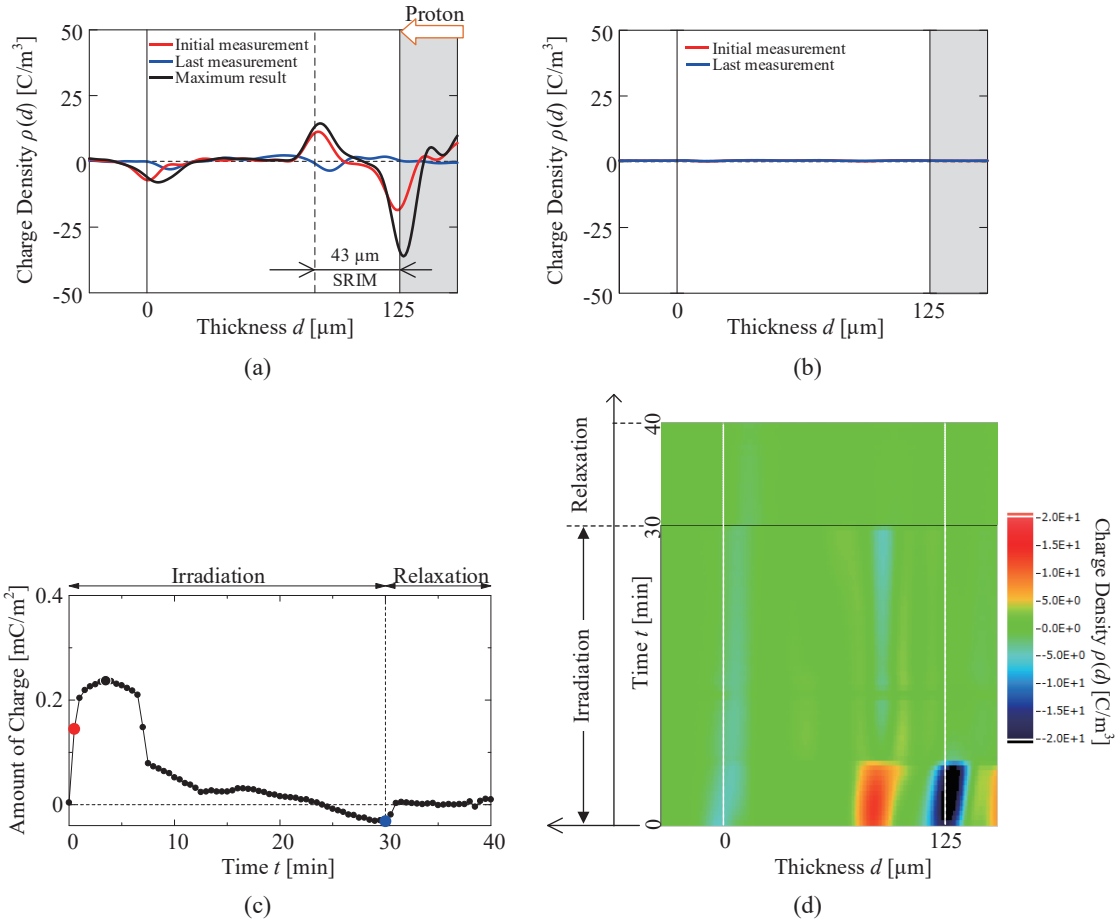

Fig. 7. (Color online) Results of space charge measurements on PMMA during and after proton beam irradiation at 1.5 MeV and 30 nA/cm^2. (a) Space charge distribution during irradiation, (b) space charge distribution after irradiation, (c) integrated accumulated positive charges in the material with time, and (d) space charge distribution with time on color chart.

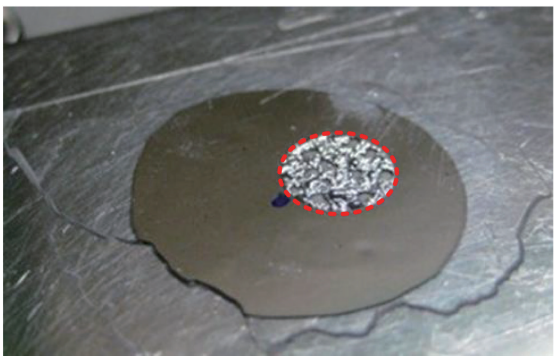

Fig. 8. (Color online) Surface erosion of PMMA due to high-current (30 nA/cm^2) proton irradiation.

6. Conclusions

We measured the charge accumulation in PMMA and quartz glass during and after proton irradiation. We observed that positive charges accumulated during proton irradiation. The position of accumulation of the positive charges was related to the proton penetration depth. However, we suggest that no charge accumulation was observed in the bulk because the injected excited secondary electrons from the Al evaporated layer moved freely toward the position of the accumulated proton and compensated for the charges of the accumulated protons.

From the results, we confirmed the measurement of the space charge distribution in dielectric materials during proton irradiation. Now we have begun to measure the space charge distribution in the materials in real spacecraft. We will publish further details in the near feature.

Acknowledgments

This study was partly supported by the Inter-University Program for the Joint Use of QST (formerly JAEA and JAERI) Facilities and the Shared Use Program of QST Facilities. This work was also supported by JSPS/MEXT KAKENHI Grant Numbers JP18760242, JP23760292, and JP15KK0216.

References

1 A. C. Tribble: The Space Environment (Princeton University Press, 1995) Chaps. 2 and 3.
2 C. Koons, J. E. Mazur, R. S. Selesnick, J. B. Blake, J. F. Fennell, J. L. Roeder, and P. C. Anderson: Proc. 6th Spacecraft Charging Technology Conf. (Air Force Research Laboratory, 1998) p. 7.
3 H. Miyake, K. Nitta, S. Michizono, and Y. Saito: J. Vac. Soc. Jpn. **50** (2007) 378.
4 H. Miyake, Y. Tanaka, and T. Takada: IEEE Trans. Dielectr. Electr. Insul. **14** (2007) 520.
5 C. Perrin, V. Griseri, and C. Laurent: IEEE Trans. Dielectr. Electr. Insul. **15** (2008) 958.
6 T. Takada: IEEE Trans. Dielectr. Electr. Insul. **6** (1999) 519.
7 T. Takada, H. Miyake, and Y. Tanaka: IEEE Trans. Plasma Sci. **34** (2006) 2176.
8 IEC/TS 62758:2012.
9 S. Maruta, H. Miyake, S. Numata, Y. Tanaka, and T. Takada: Annu. Rep. Conf. CEIDP (IEEE, 2008) p. 153.
10 J. F. Ziegler, J. P. Biersack, and U. Littmark: The Stopping and Range of Ions in Matter (Pergamon Press, New York, 1985).
11 N. W. Green and J. R. Dennison: IEEE Trans. Plasma Sci. **36** (2008) 2482.
12 G. M. Yang and G. M. Sessler: IEEE Trans. Electr. Insul. **27** (1992) 843.
13 L. Levy, T. Paulmier, B. Dirassen, C. Inguimbert, and M. V. Eesbeek: IEEE Trans. Plasma Sci. **36** (2008) 2228.
14 R. Uchiyama, T. Hara, T. Homme, H. Miyake, and Y. Tanaka: Annu. Rep. Conf. CEIDP (IEEE, 2012) 641.